Four-wave mixing dynamics of excitons in InGaAs self-assembled quantum dots

2007 J. Phys.: Condens. Matter 19 295201

(http://iopscience.iop.org/0953-8984/19/29/295201)

IOP PUBLISHING JOURNAL OF PHYSICS: CONDENSED MATTER

J. Phys.: Condens. Matter **19** (2007) 295201 (20pp) doi:10.1088/0953-8984/19/29/295201

Four-wave mixing dynamics of excitons in InGaAs self-assembled quantum dots

Paola Borri[1] **and Wolfgang Langbein**[2]

[1] School of Biosciences, Cardiff University, Cardiff CF10 3TL, UK
[2] School of Physics and Astronomy, Cardiff University, Cardiff CF24 3AA, UK

E-mail: BorriP@Cardiff.ac.uk

Received 17 April 2007
Published 11 June 2007
Online at stacks.iop.org/JPhysCM/19/295201

Abstract

In this paper we summarize our experimental work on the dephasing of excitons in self-assembled InAs/GaAs quantum dots, measured using a sensitive four-wave mixing technique in heterodyne detection. Transient four-wave mixing is a powerful technique to measure not only exciton dephasing times but also fine-structure splitting energies and exciton–biexciton binding energies which are important physical parameters for the implementation of quantum dots as source of polarization-entangled photon pairs and in the design of quantum algorithms. The scope of this paper is to review and discuss, in the context of present theories and in comparison with other experiments in the literature, the most significant results of our study on a series of thermally annealed quantum dots exhibiting systematic differences in the excitonic recombination energies and quantum confinement potentials. We will highlight the main outcomes of these measurements and give a perspective in terms of open questions that still need to be investigated, possible new experiments and potential areas of interest.

1. Introduction

The optical properties of semiconductor quantum dots (QDs) have been the subject of intense experimental and theoretical study, with tremendous progress in the last decade driven, besides fundamental interest of quantum phenomena in solid-state matter, by the wide range of possible applications of these nanostructures. Areas in which the optical response of QDs have appeared to be particularly promising in recent years include quantum electronics, optical communications, display technologies, quantum information processing and even fluorescent labelling for biological applications. Nowadays QDs can be fabricated in several ways, with the major distinction between epitaxial growth methods and chemical synthesis (sol–gel or colloidal), and exhibit a wide range of sizes and material compositions. Epitaxially grown QDs are embedded in a crystalline environment and can be directly integrated in semiconductor electrical devices, and are therefore better suited for optoelectronics applications

than chemically synthesized QDs in amorphous solid-state matrices. On the other hand, chemical fabrication is easier and less expensive than epitaxial methods. Moreover, thanks to the inherent liquid–solid interface of colloidal systems, water soluble QDs have been recently fabricated, and have opened up new, exciting perspectives in the field of bio-labelling.

Among the epitaxially grown QDs, InGaAs/GaAs QDs are probably the most widely investigated systems [1]. Their application to optical communications in the 1.3–1.5 μm wavelength window holds the promise of lower costs compared to the present InP-based technology, combined with expected superior performances arising from the reduced dimensionality. Edge-emitting InGaAs-based QD diode lasers have been demonstrated with low and temperature insensitive threshold-current densities, high output power, low linewidth enhancement factor (alpha parameter), high modulation bandwidth and long wavelength, extending to the 1.5 μm region (for recent reviews see e.g. [2, 3]). InGaAs QD-based 1.3 μm wavelength vertical-cavity surface-emitting lasers on GaAs substrates [2], optical amplifiers with high saturation power [4], broad gain bandwidth and ultrafast response [5, 6] and high-temperature infrared photodetectors have been also recently achieved [7]. Additionally, coherent light–matter interaction in QDs is receiving increasing attention due to possible solid-state implementations in the emerging field of quantum information processing. Phenomena such as resonant Rabi rotations [8, 9], cavity quantum electrodynamics in the strong coupling regime [10–12], ultralow threshold lasers [13], indistinguishable photons and polarization-entangled photons from QD single photon sources [14–17] have been recently demonstrated using InGaAs QDs as two-level systems having large transition dipole moments compared to atoms and yet narrow homogeneous linewidths compared to semiconductor structures of higher dimensionality.

Beside its fundamental interest, the knowledge of the dephasing time, inversely proportional to the homogeneous broadening, of an excitonic transition in a QD is of crucial importance for many of these applications. The dephasing time sets the time scale during which the coherence of the excitonic transition is preserved and therefore operations based on coherent-light–matter interaction can occur. Moreover, it is strictly related to intrinsic mechanisms such as radiative processes, carrier–phonon scattering and carrier–carrier scattering. Its study is a direct probe of those carrier dynamics which ultimately are limiting the high-speed performance of QD-based lasers/amplifiers.

In this paper we will present a comprehensive overview of our measurements of the dephasing processes in InAs/GaAs QDs. We investigated the temperature-dependent dephasing time in a series of thermally annealed QDs showing systematic changes in their quantum confinement potentials. We measured the dephasing dynamics of ground-state (GS) and first optically active excited-state (ES) excitonic transitions, using a sensitive transient four-wave mixing (FWM) technique in heterodyne detection. Beyond dephasing dynamics, our FWM technique combined with a polarization control of the exciting pulses resulted in a sensitive tool to measure excitonic fine-structure splittings and biexciton binding energies. These are important parameters which have recently attracted escalating attention for their relevance in the possible implementation of QDs as source of polarization-entangled photon pairs and in the design of quantum algorithms using excitons in QDs beyond single qbit operations. The scope of this paper is to review the main outcomes of our investigations and discuss them in comparison with present theories and other experiments reported in literature. At the end, we will give an outlook in terms of future work, open questions that still need to be investigated and possible new challenging experiments.

The paper is organized as follows. Section 2 describes the basic optical properties of the investigated InGaAs quantum dots and the experimental techniques utilized. Section 3 illustrates our major findings on the fine-structure splitting and exciton–biexciton binding. In

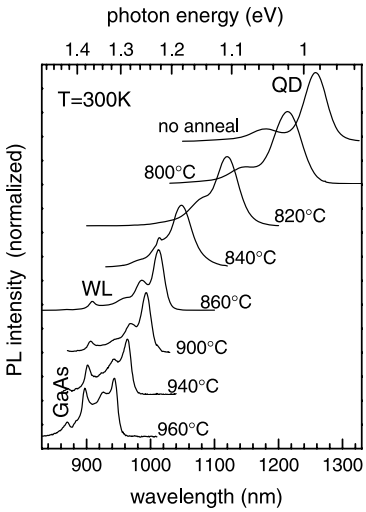

Figure 1. Non-resonantly excited photoluminescence spectra of the investigated InAs/GaAs QD sample series at room temperature. The nominal annealing temperature is given for each sample. Spectra are vertically displaced for clarity. The barrier (GaAs), wetting layer (WL) and QD transitions are indicated.

particular, their systematic changes in the QD sample series are discussed. Section 4 focuses on the dephasing processes of the GS transition, the radiative limit of the dephasing measured at low temperature is demonstrated in section 4.1 and the effect of the interaction of excitons with phonons in the temperature-dependent dephasing dynamics is extensively discussed in sections 4.2, and 4.3. Our latest experimental results on the dephasing of the ES excitonic transition are shown in section 5. Finally, a summary and outlook is given in section 6.

2. Samples and experiment

The investigated samples are planar structures containing InAs/GaAs self-assembled QDs grown on a GaAs(100) substrate using molecular-beam epitaxy. Ten stacked layers of QDs were grown separated by 100 nm GaAs spacing layers and with 2–3 $\times$ 10^{10} cm^{-2} areal density, i.e. quantum-mechanically uncoupled. QDs were obtained by deposition of a nominal coverage of 2.1 monolayers of InAs at a substrate temperature of 515 °C resulting in the formation of InAs islands that were overgrown with 8 nm GaAs at a reduced substrate temperature of 505 °C. After the growth, nine pieces of the wafer were subjected to rapid thermal annealing for 30 s at temperatures ranging from 800 to 960 °C in order to decrease the depth of the in-plane confining potential by thermally induced In diffusion in the growth direction [18]. Figure 1 shows room-temperature photoluminescence spectra under non-resonant excitation (in the GaAs barrier) for some of the samples. The lowest energy peak corresponds to the GS excitonic transition, showing a sizeable inhomogeneous and also homogeneous broadening at room temperature [19]. We observe that thermal annealing shifts the GS excitonic transition strongly to higher energies, while the wetting layer (WL) transition shifts only slightly. Therefore, the energy distance from the GS to the WL transition is tuned in the QD series from 332 to 69 meV. This energy distance will be called in the following the confinement energy E_c. Similarly, the energy separation between ES and GS is tuned in this series from $\sim$90 to 25 meV.

The FWM experiment is performed using Fourier-limited pulses of $\sim$100 fs duration at 76 MHz repetition rate, which can be tuned to be in resonance with the centre of the

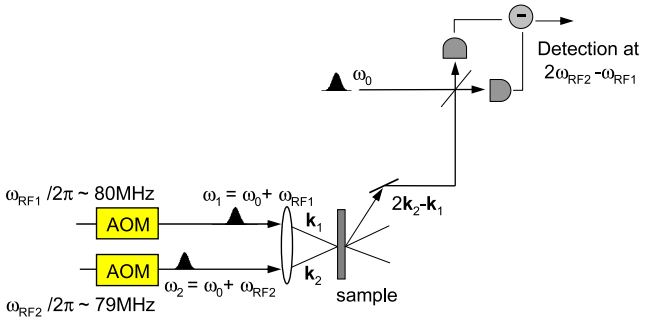

Figure 2. Sketch of the four-wave mixing set-up with directional and frequency resolved heterodyne detection. Acousto-optic modulators (AOMs) shift by a radiofrequency amount the optical frequency of the exciting pulses which are incident onto the QD sample along two different directions $\mathbf{k}_{1,2}$. The four-wave mixing signal propagating along $2\mathbf{k}_2 - \mathbf{k}_1$ interferes with an unshifted optical reference and is measured in a balanced detection scheme at the radiofrequency $2\omega_{RF2} - \omega_{RF1}$.

(This figure is in colour only in the electronic version)

inhomogeneously broadened GS or ES transitions. Two exciting pulses 1, 2 with variable relative delay time τ propagate along two different incident directions $\mathbf{k}_{1,2}$, with pulse 1 leading pulse 2 for $\tau > 0$. The FWM signal is detected along $2\mathbf{k}_2 - \mathbf{k}_1$ in transmission geometry. The intensities of the exciting pulses where chosen low enough to give rise to FWM in the third-order regime. In order to distinguish FWM intensities down to 15 orders of magnitude lower than the intensities of the transmitted beams along $\mathbf{k}_{1,2}$, we additionally used a heterodyne detection technique similar to the one discussed in our previous work [19] (see figure 2). In this technique, the pulse 1 (2) is frequency shifted by a radiofrequency ω_{RF1} (ω_{RF2}) and the interference of the FWM signal with an unshifted reference pulse is detected at $2\omega_{RF2} - \omega_{RF1}$ using high-frequency photodiodes and a lock-in amplifier [20]. In this way, the FWM field amplitude is measured via its interference with the field of the reference pulse. This detection methods reject Rayleigh scattering and photoluminescence backgrounds. Different polarization configurations of the exciting pulses and of the detected signal were chosen in the experiments, using conventional phase-retarding optics (λ-plates). The samples were antireflection coated to inhibit multiple reflections and increase light coupling and were held in a cryostat at temperatures between 5 and 120 K.

3. Beats in the four-wave mixing dynamics: fine-structure splitting and biexciton binding

Neglecting the exchange interaction, the lowest exciton level in InGaAs/GaAs QDs is four-fold spin degenerate, with two optically active states. By the short-range exchange interaction, the degeneracy between the bright and the dark exciton states is lifted, with the dark state several hundred μeV below the bright states [21]. The degeneracy between the two bright states is lifted by the long-range exchange interaction if the in-plane confinement symmetry is lowered due to structural elongation of the QDs along the [110] and [1$\bar{1}$0] crystal directions and/or strain-induced piezoelectric field [22], or even just atomistic asymmetry of the underlying lattice [23]. The resulting non-degenerate bright doublet has optical transitions linearly polarized along orthogonal directions (see scheme in figure 3). Typically, these two polarizations are along the [110] and [1$\bar{1}$0] crystal directions. In our experiment we used horizontal (x) and vertical (y) polarizations with respect to the laboratory system, which were

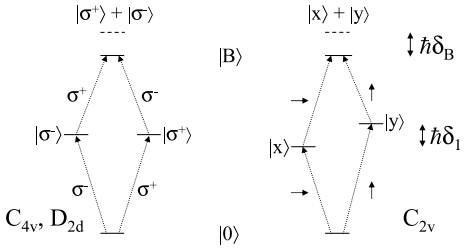

Figure 3. QD excitonic levels and polarization selection rules of the optical transitions which are important for the FWM resonant to the exciton ground state. QD ground state ($|0\rangle$), single exciton states of circular ($|\sigma^+\rangle$, $|\sigma^-\rangle$) or linear ($|x\rangle$, $|y\rangle$) basis and biexciton state ($|B\rangle$) are indicated. Left: cylindrical (D_{2d}) or square-based (C_{4v}) symmetry; right: C_{2v} symmetry.

aligned along these crystal directions indicated by the cleavage planes of the samples. The magnitude of the splitting of the two bright ground states (fine-structure splitting) and the exact influence of the physical parameters lowering the in-plane confinement symmetry have been the subject of a lively debate in recent years [24, 25, 22], also in view of the potential application of InGaAs QDs to generate polarization-entangled photon pairs for quantum information and communication. In fact, the radiative decay of the biexciton state through the two intermediate optically active states can be used to provide polarization-entangled photon pairs if the two decay path have different polarizations but are indistinguishable otherwise [17]. The fine-structure splitting results in a spectral 'which path' information that prevents the creation of polarization-entangled photons. The ability to control the exciton fine-structure splitting and eventually reduce it below the exciton radiative linewidth is thus a crucial step toward the generation of polarization-entangled photon pairs. Another important parameter for designing not only photon cascade schemes but also more complex quantum algorithms beyond single qbit operations [26–28] is the energy renormalization of the two-exciton state (biexciton binding energy) relative to twice the single exciton energy.

The fine-structure splitting is measured in the literature using polarization-dependent micro-photoluminescence spectra of single QDs [25, 22] and pump–probe transmission experiments in QD ensembles [29] including the effect of Faraday rotation [30, 31]. In our work, we used transient FWM as an alternative method. Due to its nonlinearity, polarization selection rules and phase coherence transient, FWM provided us with a direct measure of both exciton fine-structure splittings and biexciton binding energies in our thermally annealed series of QD ensembles [32].

3.1. Excitonic fine structure

Let us recall that the FWM signal of an inhomogeneously broadened QD ensemble is a photon echo in real time [19], with a time duration determined by the inhomogeneous broadening of the resonantly excited transitions, and thus similar to the exciting pulse duration. The dynamics of the microscopic polarization is probed in the delay-time dependent, time-integrated photon–echo amplitude which is shown in figure 4(left) for co-circularly polarized excitation and detection, at 5 K, on four samples with different confinement energy. As explained in detail in [32], for circularly polarized pulsed excitation, the exciton state is initially a coherent superposition of the linearly polarized states ($\sqrt{2}|\sigma^{\pm}\rangle = |x\rangle \pm \mathrm{i}|y\rangle$). The circular polarization of the exciton state after the optical excitation is oscillating in time due to the splitting energy $\hbar\delta_1$ and the corresponding quantum beats are observed in the FWM dynamics. The strong damping versus delay time is due to an inhomogeneous distribution of the fine-structure splitting within

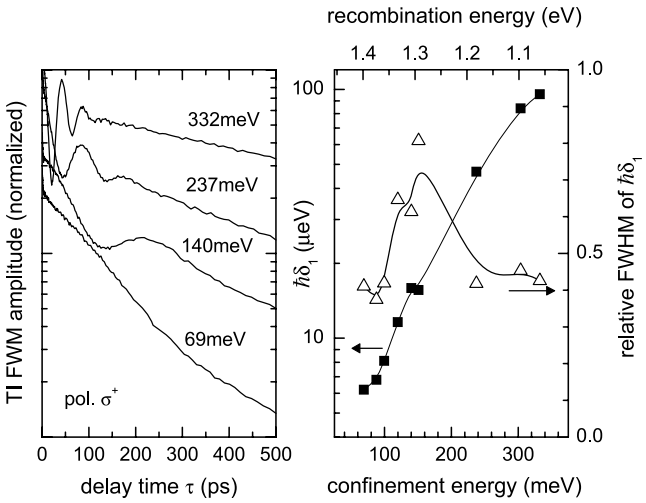

Figure 4. (Right) Time-integrated four-wave mixing amplitude at 5 K versus delay time between the exciting pulses, co-circularly polarized. Data are shown on four samples having confinement energies as indicated. (Left) Variation of the average fine-structure splitting (solid squares) and its distribution width (open triangles) over the sample series, where the effect of annealing is expressed by the confinement energy and the ground-state excitonic recombination energy at 5 K.

the ensemble. With a careful fitting procedure described in detail in [32], we extracted from the experimental data of each sample the average splitting $\hbar\delta_1$ and its relative full width at half maximum $\sqrt{8\ln 2}\sigma_1/\delta_1$, where σ_1 is the variance of the distribution of δ_1 assumed to be Gaussian.

We remark that in order to fit the data, our model had also to include a proportion (ranging from 20% to 80%) of QDs not showing fine-structure beats [32]. We attributed this proportion to charged excitons in which only a single circularly polarized transition exists and no second exciton can be excited in the electronic ground state due to Pauli blocking, which was consistent with the observation of a reduced amplitude also for the exciton–biexciton beats. This Pauli blocking picture is expected to be valid not only for negatively charged excitons but also for positively charged ones, due to the dominant heavy-hole character of the ground state excitonic transition in these strained systems and consequently negligible mixing with light-hole states. The physical origin of these charged excitons is actually unclear, since our samples are nominally undoped. It might originate from the resonant photoexcitation followed by carrier escape and separate recapture of electrons and holes into different dots, which, however, is rather unlikely at low temperature. More likely could be processes such as two-photon absorption in the barrier layer, followed by carrier capture into separate dots, or Auger ionization of the biexciton state in which one carrier can be excited in the barrier by non-radiative recombination of one electron–hole pair. Once recaptured into empty dots, single carriers can have long lifetimes at low temperature since thermal escape is a very slow process. In fact, assuming independent capture of electrons and holes of equal rate and much faster than thermal escape, we estimate that up to $2/3 = 66\%$ of dots could be singly charged.

The values of $\hbar\delta_1$ and $\sqrt{8\ln 2}\sigma_1/\delta_1$ are summarized for all samples in figure 4(right) as a function of confinement energy (which is monotonically decreasing with increasing annealing temperature). While the variance does not show a systematic trend, the average splitting decreases from 96 μeV for the sample without annealing, down to 6 μeV for the highest annealing temperature. This is in agreement with recent experimental results that show a

systematic correlation of the fine-structure splitting with the exciton recombination energy, with large splittings for low recombination energy [25, 22]. In these works, splittings are observed to even cross zero energy and invert their sign, with the sign defined by the relationship between the transition energy of the exciton line and its linear polarization direction. Although with different arguments, both works point out that strain-induced piezoelectric field must play an important role in the measured trend, rather than a structural elongation of the QDs. Due to the small In diffusion length of a few nanometres, thermal annealing is affecting the In profile mainly in the growth direction, which is the smallest dimension in these flat QDs. A symmetrization of the much larger in-plane dot shape is thus unlikely to occur with increasing annealing temperature in our series. Conversely, the strain-induced piezoelectric field is decreased by thermal annealing due to the reduced In content in the QDs. Strain gradients will even act as a driving force for directed In diffusion resulting into an In distribution of minimized strain in annealed samples. Therefore, our findings of a significant decrease of $\hbar\delta_1$ with increasing annealing temperature support the importance of piezoelectric effects, rather than structural shapes, as the physical origin for the observed fine-structure splitting.

Prior to concluding this section, we point out that while the fine-structure splitting decreases with increasing annealing temperature the radiative linewidth of the excitonic transition *increases*, as will be shown in section 4.3 (see figure 10). This trend in annealed QDs is thus promising for the generation of polarization-entangled photon pairs via the biexciton–exciton radiative cascade [17, 16].

3.2. Exciton–biexciton beats

Using a linearly polarized excitation along [110] or [1$\bar{1}$0], no fine-structure related beats are observed (see figure 7 in the next section). This is because only one of the fine-structure split states is excited. Our data indeed show a nearly perfect alignment of the optical transitions along these crystal directions. On the other hand, the biexciton can be excited, with the exciton–biexciton transition having the same linear polarization as the corresponding ground state to exciton transition (see scheme figure 3). Exciton–biexciton beats are observed in the transient FWM at small delay times due to the interference in the photon echo of the third-order polarizations in the two transitions [32]. According to the scheme in figure 3, the beat frequency $\delta_{\mathrm{B}x,\mathrm{B}y}$ is given by the energy difference between twice the exciton energy ($\hbar\omega_{x,y}$) and the biexciton energy $\hbar\omega_{\mathrm{B}}$, $\delta_{\mathrm{B}x,\mathrm{B}y} = 2\omega_{x,y} - \omega_{\mathrm{B}} = 2\omega_0 - \omega_{\mathrm{B}} \pm \delta_1 = \delta_{\mathrm{B}} \pm \delta_1$. Here we used the conventions that δ_1 is positive if state $|y\rangle$ has a higher energy than $|x\rangle$, and δ_{B} is positive if the biexciton is bound, i.e. $2\omega_0 > \omega_{\mathrm{B}}$. Since we observe no zero-crossing of δ_{B} versus annealing temperature (as will be shown in figure 6), and in annealed InAs QDs the biexciton binding energy is positive [33], we assume that δ_{B} is positive. We actually observe different beat frequencies for the two polarizations, as shown in figure 5 for the QD sample with highest confinement energy, yielding $\hbar\delta_{\mathrm{B}y} = \hbar(\delta_{\mathrm{B}} + \delta_1) \simeq 2.76$ meV, and $\hbar\delta_{\mathrm{B}x} = \hbar(\delta_{\mathrm{B}} - \delta_1) \simeq 2.53$ meV in this case. Thus $\hbar\delta_{\mathrm{B}} \simeq 2.6$ meV, and $\delta_1 \simeq 0.1$ meV, in agreement with the value $\delta_1 = 96$ μeV determined from the fine-structure beats for this sample, also confirming that $|y\rangle$ is the higher energy state.

Time-integrated FWM data showing exciton–biexciton beats versus delay at 5 K for different samples, using the same linear excitation polarization, are shown in figure 6. As in the case of the fine-structure beats, we developed a careful analysis and fitting procedure of these data versus delay to extract the values of the average biexciton binding energy $\hbar\delta_{\mathrm{B}}$ and its relative full width half maximum (assuming a Gaussian inhomogeneous distribution of binding energies) for all samples, which is also explained in detail in [32]. These results are summarized in figure 6. In the initial stage of the annealing ($E_{\mathrm{c}} > 200$ meV), $\hbar\delta_{\mathrm{B}}$ is increasing with

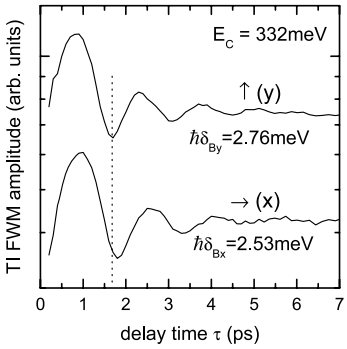

Figure 5. Time-integrated four-wave mixing amplitude at 5 K versus delay time between the exciting pulses, in the un-annealed QD sample. Linearly polarized excitation along the crystal directions was used, corresponding to horizontal (→) or vertical (↑) polarization in the laboratory system.

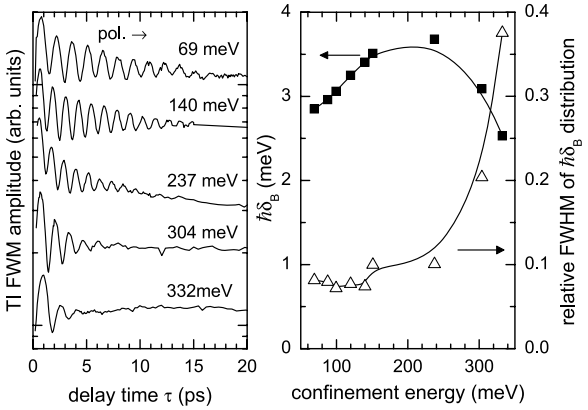

Figure 6. (Left) Time-integrated four-wave mixing amplitude at 5 K versus delay time between the exciting pulses, co-linearly polarized. Data are shown for five samples having confinement energies as indicated. (Right) Variation of the average biexciton binding energy (solid squares) and its distribution width (open triangles) over the sample series, where the effect of annealing is expressed by the confinement energy.

annealing temperature, and its inhomogeneous distribution is narrowing. For higher annealing temperatures, the inhomogeneous distribution stays constant at about 10%, suggesting that the In distribution in the growth direction has reached a diffusion-limited Gaussian shape. For such an In distribution, the electron and hole wavefunctions are inversion symmetric, minimizing the Coulomb repulsion. In this regime of stable shape, $\hbar\delta_{\mathrm{B}}$ is decreasing with decreasing confinement energy, as is expected from a theory assuming equal wavefunctions of electron and hole [34]. Conversely, the observed increase of $\hbar\delta_{\mathrm{B}}$ with decreasing confinement in the initial stage of the annealing can be explained by the shape change of the electron–hole confinement in the growth direction as follows. The In distribution of the as-grown QDs is asymmetric due to the directionality of the growth process. The consequent electron–hole charge separation [35] results in a repulsive exciton–exciton interaction, which diminishes the biexciton binding energy [36, 37]. With annealing, the In distribution tends to the Gaussian shape, reducing the repulsive interaction and thus increasing the biexciton binding energy.

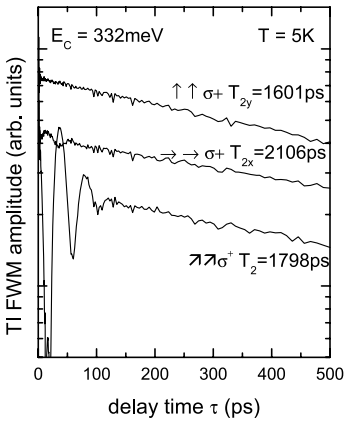

Figure 7. Time-integrated FWM field amplitude versus delay time between the exciting pulses on the un-annealed QD sample at 5 K for different linear polarizations in the excitation, as indicated. The dephasing time corresponding to the exponential decay at long delays is indicated for each polarization configuration.

Differently from the fine-structure splitting discussed in the previous section, where our findings are in agreement with a general trend as a function of the exciton recombination energy which is observed by other groups on different samples, the biexciton binding energy does not seem to follow a common trend in the literature. In the work by Young *et al* [25] they observed no correlation between the biexciton binding energy and the exciton recombination energy, different from what was reported in [38]. Additionally, in [25] they observed negative values of the biexciton binding energy for the un-annealed sample, which become positive with thermal annealing, as opposed to values not crossing zero (i.e. always positive) observed by us. We can observe a more systematic trend of the biexciton binding energy in our sample series probably because of the relatively small inhomogeneous broadening (and thus size and shape distribution) of our un-annealed sample and the systematic effect of annealing on the excitonic confinement. Let us also point out that in our un-annealed sample we observe a large inhomogeneous distribution of biexciton binding energies, rapidly reduced by thermal annealing. This suggests that the impact of the repulsive exciton–exciton interaction is very sensitive to the shape change of the electron–hole confinement in the growth direction and might result in the large scattering of biexciton binding energies reported in literature.

4. Dephasing processes

In this section we address the physical origin of the FWM dynamics for the excitonic GS transition in the temperature range from 5 to 120 K. Three main aspects emerged from this study: (i) At low, but finite, temperature the FWM decay at long delay times is in the nanosecond range, only limited by the radiative lifetime. This point is reviewed in the following subsection. (ii) Prior this long decay, the initial dynamics is characterized (even at low temperatures) by a fast non-exponential decay due to pure dephasing of excitons with acoustic phonons, giving rise to a strongly non-Lorentzian homogeneous lineshape. This will be discussed in subsection 4.2. (iii) With increasing temperature, the dephasing at long delay times is also influenced by phonon interactions, revealing a non-trivial scenario, which is discussed in subsection 4.3.

4.1. Radiatively limited dephasing

A long dephasing time is of crucial importance for the application of QDs in quantum information processing [39]. It was realized recently [19, 40, 41] that the dephasing time in InAs QDs can be as long as several hundred picoseconds at low temperature, approaching, when extrapolated to zero temperature, the nanosecond range, which is the limit set by the population lifetime. However, in these first works the measured dephasing time was always shorter than the lifetime limit even for the lowest investigated temperature (∼5 K) due to the non-negligible interaction of excitons with acoustic phonons and/or free carriers. Moreover, it was unclear if the lifetime was determined by radiative decay only, or if non-radiative decay was also significant.

In a later paper [42], we experimentally demonstrated that the dephasing time in our InAs QD series was given even at 5 K only by the *radiative* lifetime, and was up to 2 ns long, a thousand times longer than the time-scale of coherent manipulation by Rabi oscillations [43, 44]. We summarize here the main arguments of this demonstration.

As discussed in section 3.2, using linearly polarized excitation along the crystal directions one could probe the two fine-structure states separately. In this way we could measure the dephasing times of the individual optical transitions. These different times are shown in figure 7 for the un-annealed sample at 5 K. It is instructive to notice that a linearly polarized excitation along the [100] direction, which is an equal combination of the [110] and [1$\bar{1}$0] directions, exhibits strong beats similar to the circularly polarized excitation case. The radiative decay rate of each individual transition is proportional to the square of the transition dipole moment $\mu_{x,y}$, which can be different due to the spatial ellipticity of the electronic wavefunctions induced by the in-plane anisotropy of the confinement potential in the QDs. On the other hand, the FWM amplitude is proportional to the fourth power of the transition dipole moment. Therefore, we can determine the ratio between the dipole moments from the ratio of the measured FWM amplitudes. Note that in order to maintain the detection efficiency constant for this comparison, we used a $\lambda/4$-plate to filter the same circular component in the detected signal. We found that the ratio, taken at $\tau \approx 5$ ps, at which the biexciton beat has vanished but the polarization decay is negligible, was $P_y^{(3)}/P_x^{(3)} = 1.74 \pm 0.05$, yielding $\mu_y/\mu_x = 1.149 \pm 0.01$. The ratio of the radiative rates is therefore $\mu_y^2/\mu_x^2 = 1.32 \pm 0.015$, which is within error equal to the ratio of the measured dephasing times of $T_{2x}/T_{2y} = 1.316 \pm 0.005$. This comparison indicates that the measured polarization decay rates are determined by the radiative decay rates. Other dephasing processes, including spin relaxation between the exciton fine-structure states, are therefore insignificant within the measurement accuracy of 5% corresponding to dephasing times of 30 ns or longer. The lack of significant phonon-assisted dephasing at 5 K is also supported by the temperature dependence of T_{2x} which will be shown in figure 10, where an activated behaviour is found only for $T \geqslant 10$ K.

4.2. Exciton–acoustic phonon interaction: non-Lorentzian lineshape

Among the physical mechanisms responsible for the dephasing, the interaction of excitons with phonons in QDs is a topic intensively discussed in the literature and still under debate. In particular, in strongly confined epitaxially grown InGaAs/GaAs QDs an unusual non-exponential decay of the optically driven polarization was observed by us [19], corresponding to a non-Lorentzian homogeneous lineshape with a narrow line superimposed on a broad band, that has stimulated a number of theoretical works [45–54]. A clear understanding of the physical processes governing this unusual dephasing is of fundamental interest and of key importance for predicting and controlling the decoherence for applications of QDs in quantum computing.

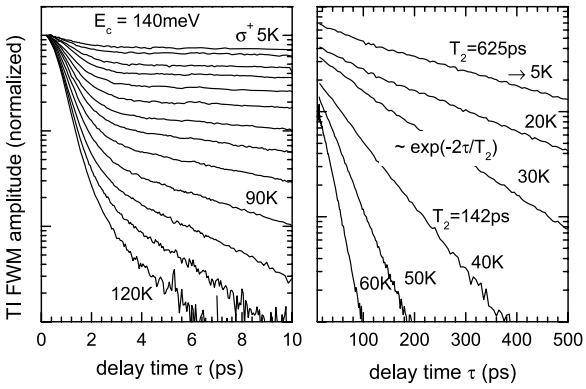

Figure 8. Time-integrated four-wave mixing field amplitude versus delay time between the exciting pulses on annealed InAs QDs with 140 meV confinement energy. Left: zoom over the initial 10 ps delay time for temperatures of 5, 10, 20 . . . 120 K in steps of 10 K. Circularly polarized excitation. Right: long delay dynamics at the indicated temperatures. Examples of the dephasing time T_2 inferred from an exponential fit according to the indicated function are also shown for the data at 5 and 40 K. Linearly polarized excitation.

Experimentally, we studied the temperature dependence of this unusual decay of the optically driven polarization [19, 55]. An example of these results for one of the annealed QD samples is shown in figure 8. With increasing temperature, the amplitude of the initial non-exponential dynamics relative to the total signal increases and the decay time of the exponential dynamics at long delays becomes shorter.

The non-exponential behaviour is explained theoretically by the independent Boson model as the manifestation in the time domain of a non-Lorentzian homogeneous lineshape with a narrow zero-phonon line (ZPL) and a broad band from pure dephasing via exciton–acoustic phonon interactions [45, 48, 50]. The amplitude increase of the initial dynamics with increasing temperature corresponds to a decrease of the weight of the ZPL versus temperature, which is well explained theoretically within this model [56, 46]. This composite non-Lorentzian lineshape is expected to be more visible in more strongly confined dots and was experimentally observed in the photoluminescence spectra of II–VI epitaxially grown QDs [56] while is hardly resolved for excitons weakly confined by the lateral disorder in narrow GaAs quantum wells [57–59].

In [60] we performed a quantitative comparison of our experimental results with the model by Vagov *et al*. This comparison is summarized in figure 9. To quantify the initial loss of coherence we determined from the experimental FWM data the fraction f by which the signal drops after the initial decay is completed. Experimental (symbols) and theoretical (lines) results for $1 - f$ which is related to the weight of the ZPL in the homogeneous lineshape are shown in figure 9(left) versus temperature for two samples as indicated. Note that f is found to be more than 20% even at low temperature. The ZPL weight decreases monotonically with rising temperature for both samples and is systematically smaller for the more strongly confined QDs, in agreement with the theory. To evaluate quantitatively the time-scale of the initial decay disentangled from the long-time behaviour we performed a normalization procedure of the data described in details in [60, 55]. Briefly, the initial dynamics was divided by the exponential decay at long delays, the asymptotic value was subtracted, and the data were renormalized to their maximum value. We then evaluated the delay time at which the normalized signal has dropped by half of its initial amplitude. The extracted times are plotted in figure 9(right) as a function of temperature for both samples. Experiments and theory confirm the tendency of

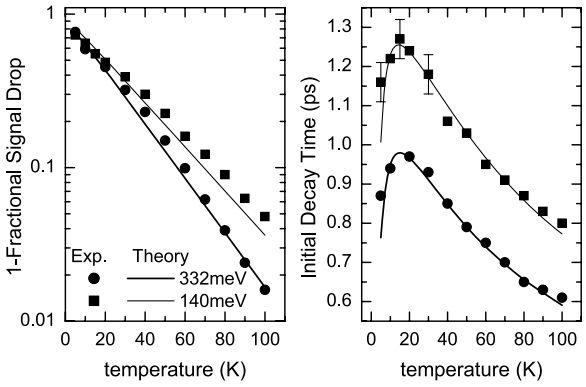

Figure 9. Comparison between experiment and theory in two QD samples with confinement energies as indicated. Symbols are the experimental data and lines are the curves calculated from the independent boson model. (Left) 1-fractional signal drop, related to the ZPL weight, as a function of temperature. (Right) Initial decoherence time versus temperature.

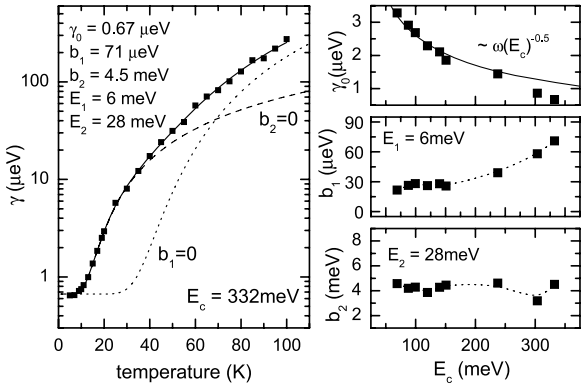

Figure 10. (Left) Homogeneous broadening (ZPL width) versus temperature (square symbols) in the un-annealed QDs together with a fit to the data (solid line) according to equation (1). The contribution of the activated term with E_1 (E_2) in equation (1) is given, including γ_0, as a dashed (dotted) line. (Right) Top: zero-temperature extrapolated width of the ZPL (square symbols) versus confinement energy compared with a curve (solid line) proportional to the inverse square root of the confinement energy E_c times the optical transition frequency ω. Middle (Bottom): coefficient b_1 (b_2) of the thermally activated increase of the ZPL width with activation energy E_1 (E_2), versus confinement energy. Dotted lines are guides to the eye. The size of the symbols is equal to or bigger than the error bars of the parameters from the fits.

a faster decoherence (i.e. a larger width of the acoustic phonon broad band) for the smaller extension of the excitonic wavefunction, present on the more strongly confined (un-annealed) dots. Moreover, a non-monotonic temperature dependence is observed. Such non-monotonic dependence, which is somewhat unusual, is well explained by the theory and is believed to be a general property of the coupling of localized electronic excitations to a continuum of vibrational modes [60].

4.3. Temperature-dependent dephasing: width of the zero-phonon line

As discussed in the previous section, the theoretical description recently proposed of the exciton–acoustic phonon interaction giving rise to a non-Lorentzian homogeneous lineshape

is able to explain the experimental observation of a decrease of the ZPL weight with increasing temperature. However, within the independent boson model the ZPL is *unbroadened*, in clear contrast to the experimentally observed broadening of the ZPL which increases with increasing temperature [19, 61]. For a theoretical description of the width of the ZPL, two types of dephasing mechanisms can be distinguished: (i) population transfer such as radiative recombination and phonon-assisted transitions toward other confined electronic levels, and (ii) pure dephasing processes that do not change the carrier occupation. In recent literature, extensions of the independent boson model with a quadratic coupling in the phonon displacement are reported in order to derive a temperature-dependent broadening of the ZPL due to pure dephasing [62, 47, 51]. However, a comparison with the experimental data using a realistic model of the dot shape is not yet available. On the other hand, our first proposed interpretation of the ZPL width in terms of inelastic dephasing processes via radiative recombination and phonon-assisted absorption into higher electronic states [19] was not supported by a systematic experimental study, e.g. as a function of the electronic energy level spacing in the QDs.

In [55] we performed a systematic experimental study of the ZPL width in the series of annealed InAs QDs. The main results of this work are summarized in figure 10. As shown in figure 8, after the initial decay over a few picoseconds, the polarization dynamics is characterized by a long exponential decay with a dephasing time T_2 inversely proportional to the width of the ZPL. In figure 10(left) the full width at half maximum $\gamma = \frac{2\hbar}{T_2}$ of the ZPL is shown versus temperature for the un-annealed QDs together with a fit to the data. We found that a good fit to the temperature dependence of γ for *all* investigated QDs was obtained using two Bose functions with activation energies E_1 and E_2 and coefficients b_1 and b_2:

$$\gamma = \gamma_0 + b_1 \frac{1}{\mathrm{e}^{E_1/k_\mathrm{B}T} - 1} + b_2 \frac{1}{\mathrm{e}^{E_2/k_\mathrm{B}T} - 1} \tag{1}$$

where γ_0 represents a temperature-independent broadening. Remarkably, the activation energies E_1 and E_2 were found to be constant within error (10%) for all investigated samples, i.e. *independent of the confinement energy*. The parameter b_2 was also roughly constant (4 ± 1 meV), while b_1 systematically increased and γ_0 decreased with increasing E_c, as shown in figure 10(right). The zero-temperature dephasing rate γ_0 is given by the radiative lifetime T_rad (i.e. $\gamma_0 = \frac{\hbar}{T_\mathrm{rad}}$, see also section 4.1), and its trend versus E_c is well understood. In fact, the radiative lifetime in InGaAs QDs depends on the electron–hole wavefunction overlap and on the exciton coherence volume [1]. Both quantities are influenced by the annealing. In particular, the reduction of the in-plane confinement potential by annealing [18] results in an increased extension of the excitonic wavefunction in-plane and thus in an increased exciton coherence area. If the in-plane exciton confinement potential is approximated by a two-dimensional harmonic oscillator potential of depth E_c (neglecting the zero-point quantization energy) reaching the wetting layer at a fixed diameter, the coherence area can be shown [42] to scale like $1/\sqrt{E_\mathrm{c}}$. Consequently the radiative decay scales like (see equations (45) and (46) in [63] or equation (5.62) in [1]) $\omega\sqrt{E_\mathrm{c}}$, where ω is the frequency of the optical transition, i.e. $\hbar\omega = E_\mathrm{WL} - E_\mathrm{c}$ with E_WL the energy of the wetting layer transition. The solid line in the top part of figure 10(right) shows this trend which well reproduces the experimental dependence for confinement energies $E_\mathrm{c} < 200$ meV. The deviation at large confinement energies could be due to an asymmetry of the In distribution in the growth direction, resulting in a decreased electron–hole wavefunction overlap and thus in a decreased radiative rate. This asymmetry is removed in the first stage of annealing. As discussed in section 3.2, measurements of the biexciton binding energy versus E_c are indeed consistent with the presence of an asymmetric In distribution in the growth direction which is symmetrized by annealing.

Concerning the temperature-dependent width of the ZPL, the activation energy $E_2 = 28$ meV is close to the range of optical phonon energies (29–36 meV) observed in InGaAs QDs [64, 65]. Optical phonons feature a density of states peaked at a certain energy. If the involved optical phonon interaction were a one-phonon absorption process, electronic excited states at the distance of the optical phonon energy would have to be present. While for confinement energies less than 100 meV, this could be due to the continuum of hole states in the wetting layer, at larger confinement energies no such continuum is expected, in contrast to the observation of a rather constant coefficient b_2 versus E_c. An alternative pure dephasing mechanism via elastic interaction with longitudinal optical phonons, which have a finite lifetime due to their decay into acoustic phonons, was discussed in [62, 47]. For a phonon lifetime smaller than the exciton dephasing time, which is the case in most of our measurements, a ZPL broadening is predicted, having a temperature dependence proportional to $\bar{n}(\bar{n}+1)$ with the phonon occupation $\bar{n}$. Since $\bar{n} \ll 1$ in the measured temperature range, this dependence is similar to the one used in equation (1). Also the observed value of b_2 is within an order of magnitude equal to the result of [62] for a similar QD structure. However, in [66] it was shown that the derivation of a finite dephasing in [62] is an artefact and that dispersionless LO phonons quadratically coupled to a single QD transition produce no broadening of the ZPL. On the other hand, the same authors of [66] have recently shown that, when all exciton levels are included in the calculations, dephasing from quadratic coupling to LO phonons is indeed present [67].

The activation energy $E_1 = 6$ meV and its coefficient b_1 are the most unexplained findings, as commented extensively in [55]. The discussion about the relevant dephasing mechanisms responsible for such temperature dependence of the ZPL width are still unsettled. It is clear, however, that our finding of a constant E_1 is in contradiction with the absorption of one acoustic phonon from the QD ground state into higher energy states, as this process should result in an activation energy given by the discrete energy-level spacing in the QDs which is systematically changing with changing confinement in our sample series. Furthermore, the experimental finding that the coefficient b_1 is increasing with increasing E_c contradicts the intuitive idea that strongly confined QDs should have a homogeneous broadening less sensitive to temperature due to inhibited phonon-assisted transitions (phonon bottleneck) between confined electronic states and further supports the importance of pure dephasing mechanisms.

Prior to concluding this section, we should remark on the lack of a relevant linear increase with temperature (aT) of the ZPL width in this QD series. As discussed in [55], the largest coefficients $a > 1$ μeV K^{-1} are reported for experiments significantly affected by dynamical broadening due to a spectral jitter of the excitonic transition. However, small but finite values of a have been observed also in experiments where dynamical broadening is strongly reduced. In our previous work using transient FWM [19], we measured $a = 0.22$ μeV K^{-1}. The zero-temperature extrapolated ZPL broadening was consistent with the lifetime limit, so that we could exclude a significant influence of dynamical broadening. There, we attributed a to phonon-assisted transitions among the exciton fine-structure states. However, this interpretation appears to contradict recent measurements showing an exciton spin–flip time much longer than the radiative lifetime [68], as we also deduced in section 4.1. Since the sample investigated in [19] was in a p-i-n diode allowing for electrical injection, we now believe that the vicinity of QDs to free carriers in the doped cladding layers and the consequent Coulomb interaction is more likely to explain the measured a in that sample.

5. Dephasing of excited-state excitons

Beside their application to lasers and amplifiers, QDs have recently been considered to show superior performances as variable all-optical buffers exploiting slow light via

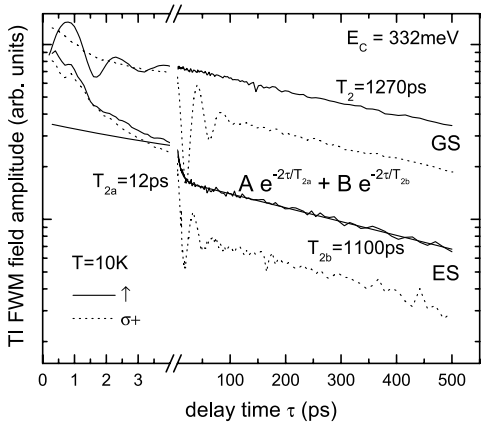

Figure 11. Time-integrated FWM field amplitude versus delay between the exciting pulses on the un-annealed InAs QDs at 10 K for the ground state (GS) and first optically active excited state (ES) excitonic transition, separated by 90 meV, in two polarization configurations (circular ($\sigma+$) and vertically linear ($\uparrow$)). A bi-exponential fit to the ES decay is indicated with the corresponding values of the dephasing time.

electromagnetically induced transparency (EIT) [69], a phenomenon intrinsically limited by the dephasing of QD optical transitions, including the excited states. A long dephasing time of the first excited state excitonic transition would therefore be very useful to exploit EIT with QDs, and more generally for flexible and alternative schemes of coherent manipulation involving not only the GS quantum bit.

We have recently reported transient FWM measurements of the first optically active ES excitonic transition for strongly confined (un-annealed) InAs QDs in comparison with calculations by Muljarov and Zimmermann [70, 71], while a systematic study on the series of annealed QDs is in progress and will be reported elsewhere. The main experimental findings are summarized in figures 11 and 12. In figure 11 the time-integrated FWM field amplitude versus delay between the exciting pulses is shown at 10 K for both GS and ES transitions for circular and linear polarization configurations. The initial dynamics over a few picoseconds exhibits the fast decay characteristic of the pure dephasing from the broad acoustic-phonon band, well explained by the independent boson model and discussed in section 4.2. After this initial dynamics, however, the optically induced ES polarization decays bi-exponentially, as shown by the fit in figure 11. Remarkably, a significant component of the ES signal shows a long dephasing time $T_{2B} = 1.1$ ns, comparable to the long GS dephasing associated with the ZPL width.

An obvious doubt about this surprisingly slow ES dephasing (experimental ES dephasing times reported in literature to date do not exceed 90 ps in InGaAs/GaAs QDs [72]) is that we might sill probe a subgroup of the inhomogeneously broadened GS transitions with a long dephasing time even when measuring in resonance with the ES transitions. To check this hypothesis we have compared the photoluminescence (PL) spectrum with the amplitude B of the slow dephasing component for different wavelengths in the range from GS to ES, as shown in figure 12. Due to the random capture of the non-resonantly excited carriers at low temperature, the PL spectrum for low excitation intensity is a probe of the distribution of GS transition energies (assuming fast intradot relaxation). If B is due to the GS distribution, it should then scale accordingly (note that in our experiment we are sensitive to the FWM amplitude which is directly proportional to the number of microscopic dipoles contributing

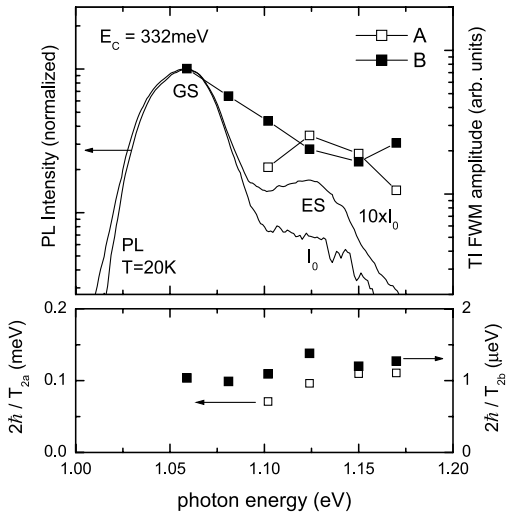

Figure 12. Top: photoluminescence spectrum at 20 K of the un-annealed InAs QDs for non-resonant excitation (at 1.959 eV) with low (I_0) and 10 times higher excitation intensity, compared with the amplitudes of the bi-exponential ES dephasing. The amplitude A is found to be zero below 1.10 eV. Bottom: homogeneous linewidth corresponding to the fast (open squares) and slow (closed squares) dephasing of the ES at 10 K.

to the macroscopic polarization). Conversely, we found that B is much higher than the contribution from GS transitions at the ES wavelength, and is also comparable to the amplitude A of the fast dephasing component. We therefore conclude that a significant portion of ES transitions indeed exhibit a long dephasing time, nearly radiative lifetime limited, in our QD sample.

Preliminary calculations by Muljarov and Zimmermann could explain qualitatively the observed bi-exponential behaviour and the long ES dephasing component [70, 71]. These calculations consider a multilevel excitonic system coupled to acoustic phonons, with two bright excitonic excited states being non-degenerate in the absence of in-plane cylindrical symmetry, even neglecting the spin components, simply due to a spatial wavefunction anisotropy. Briefly, the bi-exponential decay reflects two different dephasing rates of the two bright states, with the lower bright state being considerably far in energy from other states to have a long dephasing time mainly due to virtual transitions, while the upper state is always closer to one of the dark states and thus has a much faster dephasing due to real acoustic–phonon transitions. However, compared with the experiment, the calculated bi-exponential decay has one major discrepancy: the amplitude of the fast dephasing component is one order of magnitude smaller than the amplitude of the slow dephasing term, due to the small oscillator strength of the upper bright state. In order to overcome this discrepancy, calculations are in progress to include the second excited levels (so called d-states), especially for the holes, which were shown to contribute to a Coulomb mixing and splitting of the p-shell with redistribution of the oscillator strength [73].

We should comment that the measured long ES dephasing time also implies a strongly inhibited LO-phonon-assisted relaxation of ES, somewhat in contradiction with recent measurements of the intraband electron relaxation via polaron decay, which show relaxation times of no longer than 70 ps [74]. On the other hand, time-resolved photoluminescence measurements of the excitonic relaxation from ES to GS in InAs QDs were performed in [75]

and showed the occurrence of a strongly inhibited relaxation, consistent with the long dephasing measured by us. One should also comment that a proper theory of the ES excitonic relaxation and dephasing, including virtual and real transitions with acoustic and optical phonons and taking into account detailed information of the QD shape, is still missing.

In conclusion, at this stage the interpretation of the measured long ES exciton dephasing times in our InAs QDs appears controversial, and is open to more experimental and theoretical work.

6. Summary and outlook

In summary, we have reviewed our most important experimental findings of the ground-state excitonic fine-structure splitting, biexciton binding energy, as well as ground and excited state exciton dephasing time, with its temperature dependence, in a series of thermally annealed InAs quantum dots. For the application of InAs QDs to generate polarization-entangled photon pairs, this study has shown the useful role of thermal annealing in significantly reducing the fine-structure splitting (from 96 to 6 μeV) while increasing the exciton radiative linewidth (from 0.67 to 3.3 μeV). The major role of lattice anisotropy effects, such as strain-induced piezoelectric fields, in reducing the in-plane symmetry of the confining potential, and thus giving rise to a fine-structure splitting, was also pointed out. Conversely, thermal annealing changed the biexciton binding energy in a non-monotonic way and only by 1 meV around a value of $\sim$3 meV, while having major impact on the inhomogeneous distribution of biexciton binding energies which was found to significantly reduce from almost 40% to less 10% with annealing. This reduced inhomogeneous distribution, together with an energetically well separated transition energy, could make feasible the application of the exciton–biexciton transition for two qbit operations even in QD ensembles. In relation to that, it is interesting to recall that experiments with Rabi oscillations in InGaAs QDs showed the presence of an inhomogeneous distribution of transition dipole moments playing a major role in damping these oscillations in QD ensembles [8]. It would be instructive to investigate if such an inhomogeneous distribution of transition dipole moments is also reduced by thermal annealing. This could lead to the interesting possibility of observing several Rabi rotations in QD ensembles, up to now reported only in single QDs [76], and could potentially lead to improved coherent phenomena involving propagation effects such as self-induced transparency [77].

Our finding of a radiatively limited dephasing of the zero-phonon line in QDs, even at finite (5 K) temperature, is very promising, because if the homogeneous lineshape were given by the ZPL only, coherent-light–matter interaction in these systems would last as long as the radiative decay, without disruptive effects from pure dephasing. This is also very important for generating indistinguishable photons from single QDs [78]. On the other hand our work demonstrated, in agreement with the independent boson model, that even at low temperatures the zero-phonon line is superimposed on a broad acoustic phonon band, especially for strongly localized dots, corresponding to an initial non-exponential decoherence from pure dephasing by acoustic-phonon interaction. Thermal annealing again plays a useful role by reducing the strength of quantum confinement and thus increasing the weight of the ZPL at a given temperature. However, this effect is significant at high temperature ($>$20 K). At 5 K about 20% of the initial FWM amplitude is already lost after few picoseconds (corresponding to a ZPL weight of $\sim$0.9 [55]) in all thermally annealed QDs investigated by us. It has been suggested recently that the detrimental effect of such decoherence during an operation performed by a sequence of a fixed number of pulses can be significantly reduced by using pulses of finite duration optimized so that the spectral overlap with phonon modes is minimized [53].

Concerning the temperature dependence of the ZPL width, there is clearly the need to go beyond the independent boson model; however, the comparison of our experimental findings with theory is still partly unsettled. Our results point towards pure dephasing mechanisms playing a major role, rather than one-phonon absorption processes. A ZPL width from pure dephasing is explained in the theory via a quadratic coupling to both acoustic and optical phonons. However, quantitative modelling, especially concerning the coupling with acoustic phonons, is still missing. In addition to this open discussion comes our most recent finding of a surprisingly long dephasing (in the nanosecond range at 10 K) of the excitonic first excited state. On the one hand this result is consistent with the lack of significant one-phonon absorption/emission processes between ground and excited states, as suggested by our measurement of the temperature dependence of the ZPL width; on the other it contradicts recent reports of a relatively fast intraband electron relaxation via polaron decay, and it is also not yet explained quantitatively by the theory.

To clarify this unsettled scenario, more effort needs to be made both experimentally and theoretically. From the experimental side, great benefit will come from the possibility recently opened by Langbein *et al* [79–82] to perform transient FWM in single QDs, and thus to clearly distinguish between processes occurring within one dot from those occurring in different dots and averaged in the ensemble response. The ability to perform this type of measurement in single InAs QDs is challenging, and results have been reported up to now only on excitons weakly localized by interface fluctuations in disordered GaAs quantum wells, and in CdTe QDs. It would also be important and instructive to measure the ES dephasing in doped QDs, to test the possible role of spin-blockade of charged excitons in the measured long dephasing dynamics. From the point of view of the theory, effort still needs to be made toward a complete model of the ES and GS excitonic dephasing including virtual and real transitions with acoustic and optical phonons.

Acknowledgments

Access to experimental facilities in the Physics Department of Dortmund University, Germany, in the group of Professor U Woggon, is acknowledged. Samples were grown by D Reuter and A D Wieck, Bochum University, Germany.

References

[1] Bimberg D, Grundmann M and Ledentsov N N 1999 *Quantum Dot Heterostructures* (Chichester: Wiley)
[2] Ledentsov N N 2002 *IEEE J. Sel. Top. Quantum Electron.* **8** 1015
[3] Bimberg D 2005 *J. Phys. D: Appl. Phys.* **38** 2055
[4] Berg T W and Mørk J 2004 *IEEE J. Quantum Electron.* **40** 1527
[5] Borri P, Langbein W, Hvam J M, Heinrichsdorff F, Mao M-H and Bimberg D 2000 *J. Sel. Top. Quantum Electron.* **6** 544
[6] Sugawara M, Ebe H, Hatori N, Ishida M, Arakawa Y, Akiyama T, Otsubo K and Nakata Y 2004 *Phys. Rev.* B **69** 235332
[7] Chakrabarti S, Stiff-Roberts A D, Su X H, Bhattacharya P, Ariyawansa G and Perera A G U 2005 *J. Phys. D: Appl. Phys.* **38** 2135
[8] Borri P, Langbein W, Schneider S, Woggon U, Sellin R L, Ouyang D and Bimberg D 2002 *Phys. Rev.* B **66** 081306(R)
[9] Zrenner A, Beham E, Stufler S, Findeis F, Bichler M and Abstreiter G 2002 *Nature* **418** 612
[10] Reithmaier J P, Sęk G, Löffler A, Hoffmann C, Kuhn S, Reitzenstein S, Keldysh L V, Kulakovskii V D, Reinecke T L and Forchel A 2004 *Nature* **432** 197
[11] Yoshie T, Scherer A, Hendrickson J, Khitrova G, Gibbs H M, Rupper G, Ell C, Shchekin O B and Deppe D G 2004 *Nature* **432** 200
[12] Peter E, Senellart P, Martrou D, Lemaître A, Hours J, Gérard J M and Bloch J 2005 *Phys. Rev. Lett.* **95** 067401

[13] Strauf S, Hennessy K, Rakher M T, Choi Y-S, Badolato A, Andreani L C, Hu E L, Petroff P M and Bouwmeester D 2006 *Phys. Rev. Lett.* **96** 127404
[14] Santori C, Fattal D, Vuckovic J, Solomon G S and Yamamoto Y 2002 *Nature* **419** 594
[15] Fattal D, Inoue K, Vuckovic J, Santori C, Solomon G S and Yamamoto Y 2004 *Phys. Rev. Lett.* **92** 037903
[16] Stevenson R M, Young R J, Atkinson P, Cooper K, Ritchie D A and Shields A J 2006 *Nature* **439** 179
[17] Akopian N, Lindner N H, Poem E, Berlatzky Y, Avron J, Gershoni D, Gerardot B D and Petroff P M 2006 *Phys. Rev. Lett.* **96** 130501
[18] Fafard S and Allen C N 1999 *Appl. Phys. Lett.* **75** 2374
[19] Borri P, Langbein W, Schneider S, Woggon U, Sellin R, Ouyang D and Bimberg D 2001 *Phys. Rev. Lett.* **87** 157401
[20] Borri P 2002 *Nano-Optoelectronics: Concepts, Physics and Devices, Nanoscience and Technology* ed M Grundmann (Berlin: Springer) pp 411–30
[21] Bayer M *et al* 2002 *Phys. Rev.* B **65** 195315
[22] Seguin R, Schliwa A, Rodt S, Pötschke K, Pohl U W and Bimberg D 2005 *Phys. Rev. Lett.* **95** 257402
[23] Bester G, Nair S and Zunger A 2003 *Phys. Rev.* B **67** 161306(R)
[24] Seidl S, Kroner M, Högele A, Karrai K, Warburton R J, Badolato A and Petroff P M 2006 *Appl. Phys. Lett.* **88** 203113
[25] Young R J, Stevenson R M, Shields A J, Atkinson P, Cooper K, Ritchie D A, Groom K M, Tartakovskii A I and Skolnick M S 2005 *Phys. Rev.* B **72** 113305
[26] Piermarocchi C, Chen P, Dale Y S and Sham L J 2002 *Phys. Rev.* B **65** 075307
[27] Li X, Wu Y, Steel D, Gammon D, Stievater T H, Katzer D S, Park D, Piermarocchi C and Sham L J 2003 *Science* **301** 809
[28] Stufler S, Machnikowski P, Ester P, Bichler M, Axt V M, Kuhn T and Zrenner A 2006 *Phys. Rev.* B **73** 125304
[29] Tartakovskii A I *et al* 2004 *Phys. Rev. Lett.* **93** 057401
[30] Greilich A, Schwab M, Berstermann T, Auer T, Oulton R, Yakovlev D R and Bayer M 2006 *Phys. Rev.* B **73** 045323
[31] Bernardot F, Aubry E, Tribollet J, Testelin C, Chamarro M, Lombez L, Braun P-F, Marie X, Amand T and Gérard J-M 2006 *Phys. Rev.* B **73** 085301
[32] Langbein W, Borri P, Woggon U, Stavarache V, Reuter D and Wieck A D 2004 *Phys. Rev.* B **69** 161301(R)
[33] Finley J J, Ashmore A D, Lemaître A, Mowbray D J, Skolnick M S, Itskevich I E, Maksym P A, Hopkinson M and Krauss T F 2001 *Phys. Rev.* B **63** 073307
[34] Bryant G W 1990 *Phys. Rev.* B **41** 1243
[35] Barker J A and OReilly E P 2000 *Phys. Rev.* B **61** 13840
[36] Shumway J, Franceschetti A and Zunger A 2001 *Phys. Rev.* B **63** 155316
[37] Stier O, Heitz R, Schliwa A and Bimberg D 2002 *Phys. Status Solidi* a **190** 477
[38] Rodt S, Schliwa A, Pötschke K, Guffarth F and Bimberg D 2005 *Phys. Rev.* B **71** 155325
[39] Knill E, Laflamme R and Milburn G 2001 *Nature* **409** 46
[40] Birkedal D, Leosson K and Hvam J M 2001 *Phys. Rev. Lett.* **87** 227401 1
[41] Bayer M *et al* 2002 *Phys. Rev.* B **65** 195315
[42] Langbein W, Borri P, Woggon U, Stavarache V, Reuter D and Wieck A D 2004 *Phys. Rev.* B **70** 033301
[43] Borri P, Langbein W, Schneider S, Woggon U, Sellin R L, Ouyang D and Bimberg D 2002 *Phys. Rev.* B **66** 081306(R)
[44] Htoon H, Tagakahara T, Kulik D, Baklenov O, Holmes A L Jr and Shih C K 2002 *Phys. Rev. Lett.* **88** 087401
[45] Krummheuer B, Axt V M and Kuhn T 2002 *Phys. Rev.* B **65** 195313
[46] Zimmermann R and Runge E 2002 *Proc. of the 26th Int. Conf. on Physics of Semiconductors* ed J H Davies and A R Long (UK: Institute of Physics Publishing) p M3.1
[47] Goupalov S V, Suris R A, Lavallard P and Citrin D S 2002 *IEEE J. Sel. Top. Quantum Electron.* **8** 1009
[48] Vagov A, Axt V M and Kuhn T 2002 *Phys. Rev.* B **66** 165312 1
[49] Förstner J, Weber C, Danckwerts J and Knorr A 2003 *Phys. Rev. Lett.* **91** 127401
[50] Vagov A, Axt V M and Kuhn T 2003 *Phys. Rev.* B **67** 115338
[51] Muljarov E A and Zimmermann R 2004 *Phys. Rev. Lett.* **93** 237401
[52] Krummheuer B, Axt V M, Kuhn T, D'Amico I and Rossi F 2005 *Phys. Rev.* B **71** 235329
[53] Axt V M, Machnikowski P and Kuhn T 2005 *Phys. Rev.* B **71** 155305
[54] Krügel A, Axt V M and Kuhn T 2006 *Phys. Rev.* B **73** 035302
[55] Borri P, Langbein W, Woggon U, Stavarache V, Reuter D and Wieck A D 2005 *Phys. Rev.* B **71** 115328
[56] Besombes L, Kheng K, Marsal L and Mariette H 2001 *Phys. Rev.* B **63** 155307
[57] Guest J, Stievater T H, Chen G, Tabak E A, Orr B G, Steel D G, Gammon D and Katzer D S 2001 *Science* **293** 2224

[58] Peter E, Hours J, Senellart P, Vasanelli A, Cavanna A, Bloch J and Gérard J M 2004 *Phys. Rev.* B **69** 041307(R)
[59] Mannarini G and Zimmermann R 2006 *Phys. Rev.* B **73** 115325
[60] Vagov A, Axt V M, Kuhn T, Langbein W, Borri P and Woggon U 2004 *Phys. Rev.* B **70** 201305(R)
[61] Bayer M and Forchel A 2002 *Phys. Rev.* B **65** 041308
[62] Uskov A V, Jauho A-P, Tromborg B, Mørk J and Lang R 2000 *Phys. Rev. Lett.* **85** 1516
[63] Sugawara M 1995 *Phys. Rev.* B **51** 10743
[64] Heitz R, Veit M, Ledentsov N N, Hoffmann A, Bimberg D, Ustinov V M, Kop'ev P S and Alferov Z I 1997 *Phys. Rev.* B **56** 10435
[65] Heitz R, Born H, Hoffmann A, Bimberg D, Mukhametzhanov I and Madhukar A 2000 *Appl. Phys. Lett.* **77** 3746
[66] Muljarov E A and Zimmermann R 2006 *Phys. Rev. Lett.* **96** 019703
[67] Muljarov E A and Zimmermann R 2006 *Preprint* cond-mat/0605545
[68] Paillard M, Marie X, Renucci R, Amand T, Jbeli A and Gérard J M 2001 *Phys. Rev. Lett.* **86** 1634
[69] Ku P, Chang-Hasnain C J and Chuang S L 2002 *Electron. Lett.* **38** 1581
[70] Muljarov E A and Zimmermann R 2006 *Phys. Status Solidi* b **243** 2252
[71] Borri P, Langbein W, Muljarov E A and Zimmermann R 2006 *Phys. Status Solidi* b **243** 3890
[72] Htoon H, Kulik D, Baklenov O, Holmes A L Jr, Takagahara T and Shih C K 2001 *Phys. Rev.* B **63** 241303
[73] Bayer M, Forchel A, Hawrylak P, Fafard S and Narvaez G 2001 *Phys. Status Solidi* b **224** 331
[74] Zibik E A *et al* 2004 *Phys. Rev.* B **70** 161305(R)
[75] Heitz R, Born H, Guffarth F, Stier O, Schliwa A, Hoffmann A and Bimberg D 2001 *Phys. Rev.* B **64** 241305(R) 1
[76] Stufler S, Ester P, Zrenner A and Bichler M 2005 *Phys. Rev.* B **72** 121301(R)
[77] Schneider S, Borri P, Langbein W, Woggon U, Förstner J, Knorr A, Sellin R L, Ouyang D and Bimberg D 2003 *Appl. Phys. Lett.* **83** 3668
[78] Varoutsis S, Laurent S, Kramper P, Lemaître A, Sagnes I, Robert-Philip I and Abram I 2005 *Phys. Rev.* B **72** 041303(R)
[79] Langbein W and Patton B 2005 *Phys. Rev. Lett.* **95** 017403
[80] Patton B, Woggon U and Langbein W 2005 *Phys. Rev. Lett.* **95** 266401
[81] Langbein W and Patton B 2006 *Opt. Lett.* **31** 1151
[82] Patton B, Langbein W, Woggon U, Maingault L and Mariette H 2006 *Phys. Rev.* B **73** 235354